Supplemental Material

© Copyright 2020 American Meteorological Society
Permission to use figures, tables, and brief excerpts from this work in scientific and educational works is hereby granted provided that the source is acknowledged. Any use of material in this work that is determined to be “fair use” under Section 107 of the U.S. Copyright Act or that satisfies the conditions specified in Section 108 of the U.S. Copyright Act (17 USC §108) does not require the AMS’s permission. Republication, systematic reproduction, posting in electronic form, such as on a website or in a searchable database, or other uses of this material, except as exempted by the above statement, requires written permission or a license from the AMS. All AMS journals and monograph publications are registered with the Copyright Clearance Center (http://www.copyright.com). Questions about permission to use materials for which AMS holds the copyright can also be directed to permissions@ametsoc.org. Additional details are provided in the AMS Copyright Policy statement, available on the AMS website (http://www.ametsoc.org/CopyrightInformation).

Supporting information for

Sensitivities and responses of land surface temperature to deforestation-induced biophysical changes in two global earth system models

Contents of this file

Figures S1 to S12

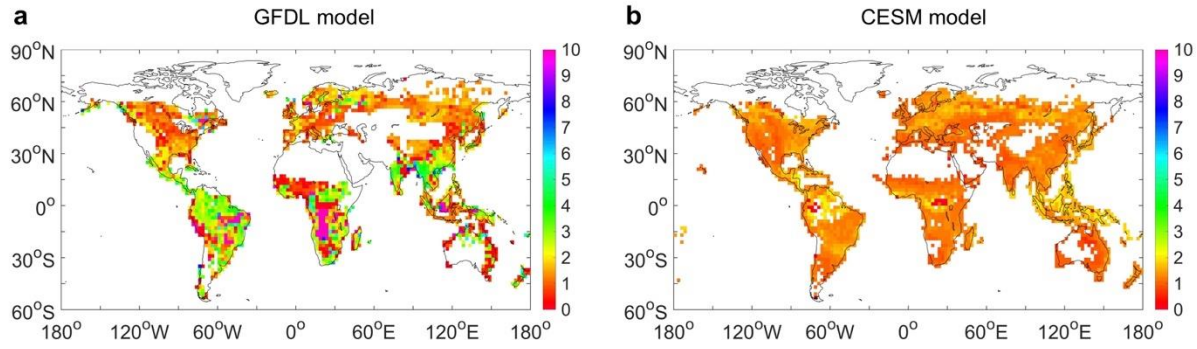

FIG. S1. The optimized values for *m* in (a) the GFDL ESM2Mb and (b) the CESM models.

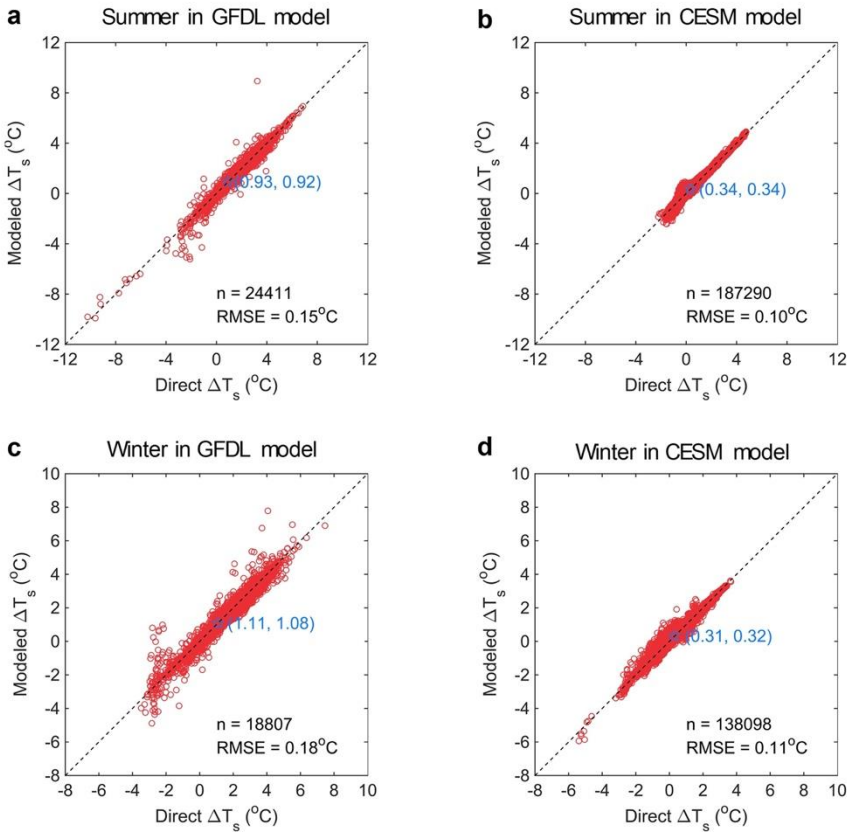

FIG. S2. Comparisons between the direct ΔT_s computed by the GFDL ESM2Mb and the CESM models and the modeled ΔT_s computed by the attribution methods in summer and winter. The blue stars and values denote the mean values.

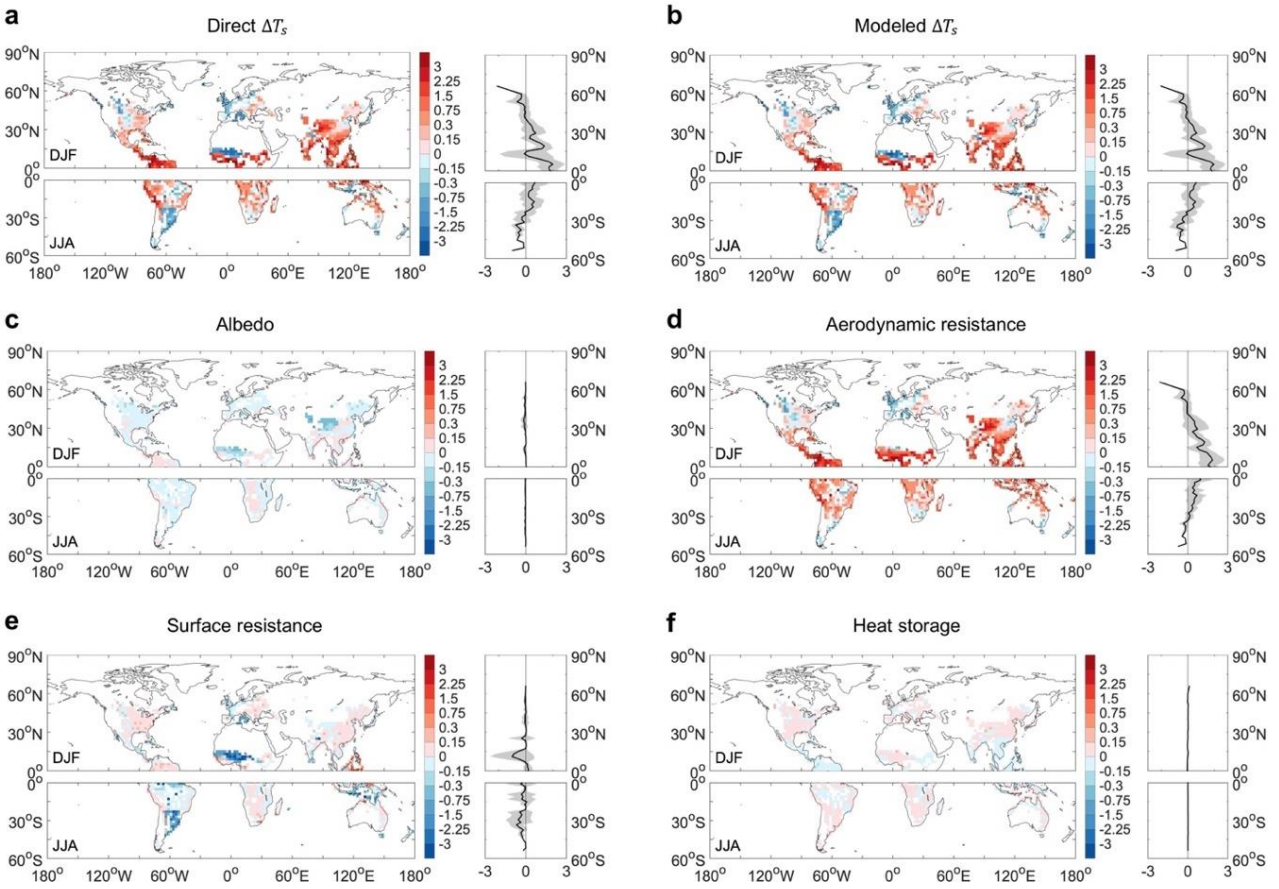

FIG. S3. Attribution of the LST contrast between forests and croplands (Δ = cropland – forest) during winter in the GFDL ESM2Mb model. (a) The direct ΔT_s calculated by taking the temperature difference between forests and croplands in the GFDL ESM2Mb model simulation and (b) the modeled ΔT_s computed by the attribution method. Contributions to the LST contrast from changes in the (c) albedo, (d) aerodynamic resistance, (e) surface resistance, and (f) heat storage based on the attribution method. Panel (b) corresponds to the term on the l.h.s. of Eq. (19) while panels (c-f) correspond to, in order, the terms on the r.h.s. of Eq. (19). For the Northern and Southern Hemispheres, the figure shows the DJF and JJA averages, respectively. The black line denotes the latitudinal dependence of the corresponding value and the gray shading represents the mean ± standard deviation of the corresponding value. Units are ºC.

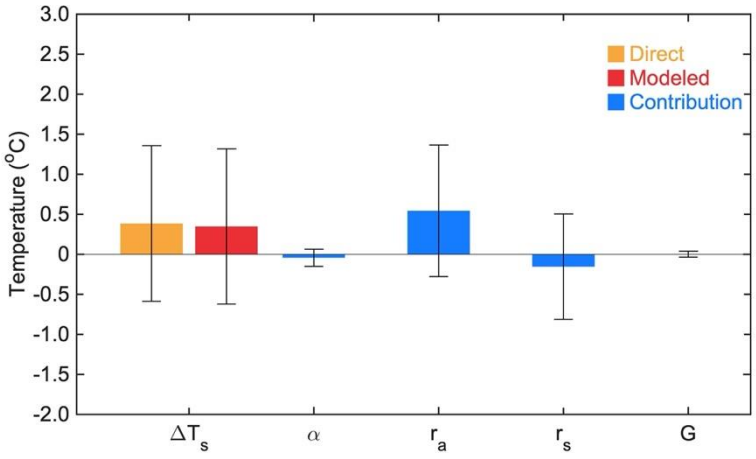

FIG. S4. Global averages of the attribution results for the LST contrast between forests and croplands (Δ = cropland – forest) during winter in the GFDL ESM2Mb model. The yellow bar donates the directly ΔT_s calculated by taking the temperature difference between forests and croplands, the red bar denotes the modeled ΔT_s computed by the attribution method, and the blue bars denote the contributions from different biophysical factors. The error bars are given as the standard deviation of the global mean and indicate the spatial variability.

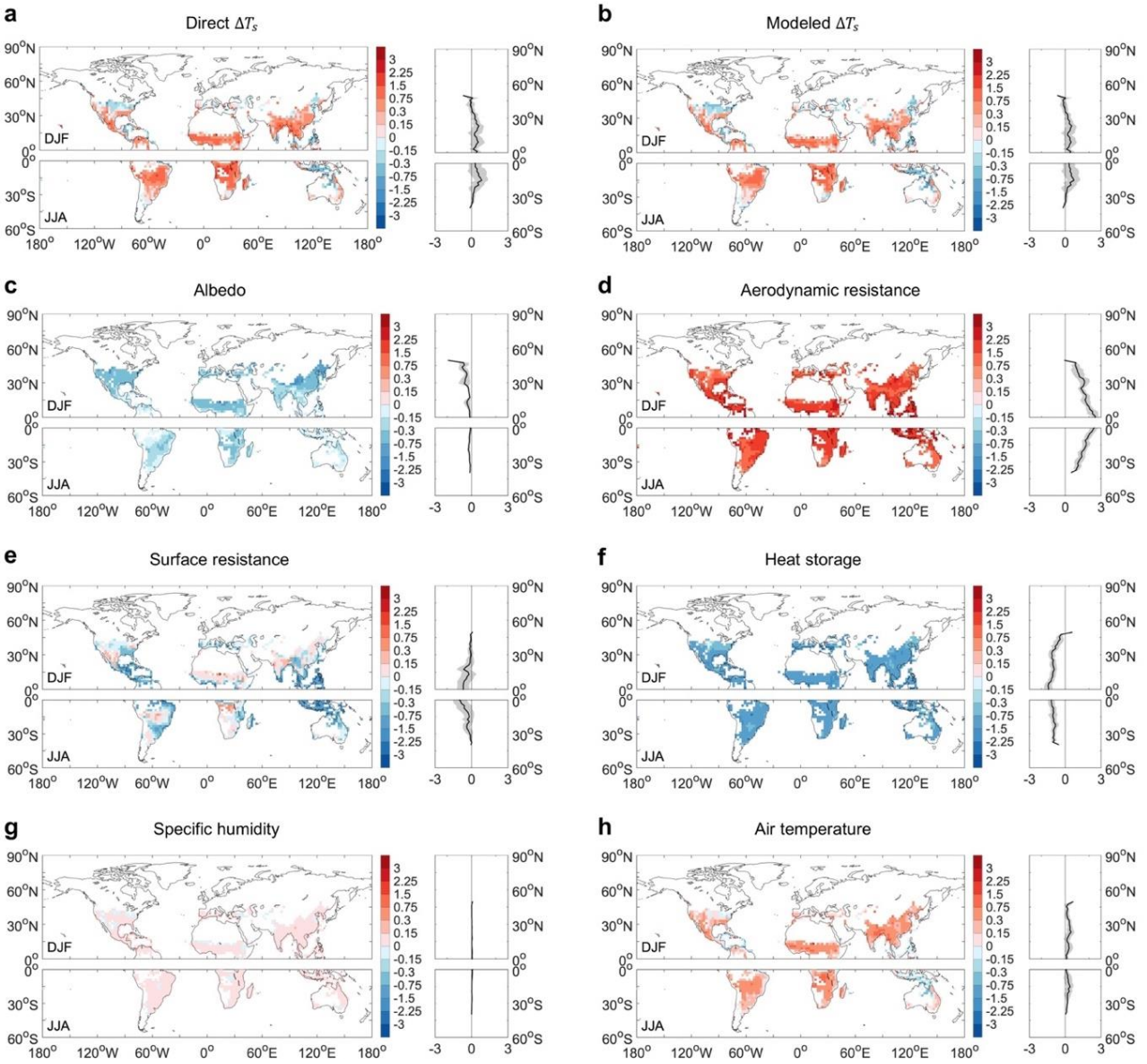

FIG. S5. Attribution of the LST contrast between forests and croplands (Δ = cropland – forest) during winter in the CESM model. (a) The direct ΔT_s calculated by taking the temperature difference between forests and croplands in the CESM model simulation and (b) the modeled ΔT_s computed by the attribution method. Contributions to the LST contrast from changes in the (c) albedo, (d) aerodynamic resistance, (e) surface resistance, (f) heat storage, (g) specific humidity, and (h) air temperature based on the attribution method. Panel (b) corresponds to the term on the l.h.s. of Eq. (20) while panels (c-h) correspond to, in order, the first six terms on the r.h.s. of Eq. (20). For the Northern and Southern Hemispheres, the figure shows the DJF and JJA averages, respectively. The black line denotes the latitudinal dependence of the corresponding value and the gray shading represents the mean ± standard deviation of the corresponding value. Units are ºC.

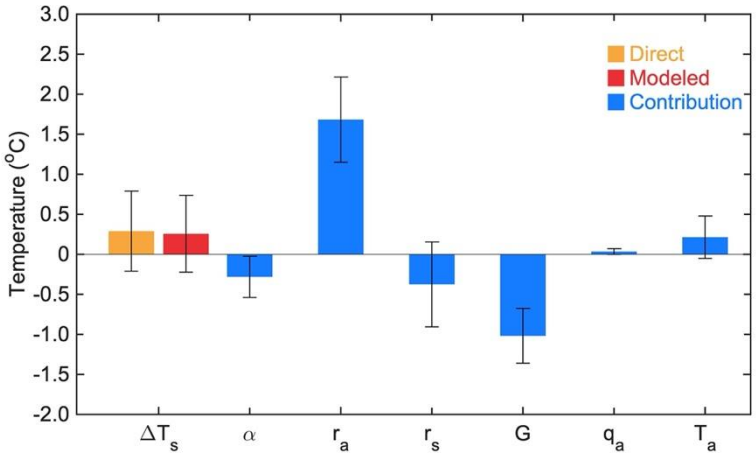

FIG. S6. Similar to Fig. S4 but with the CESM model.

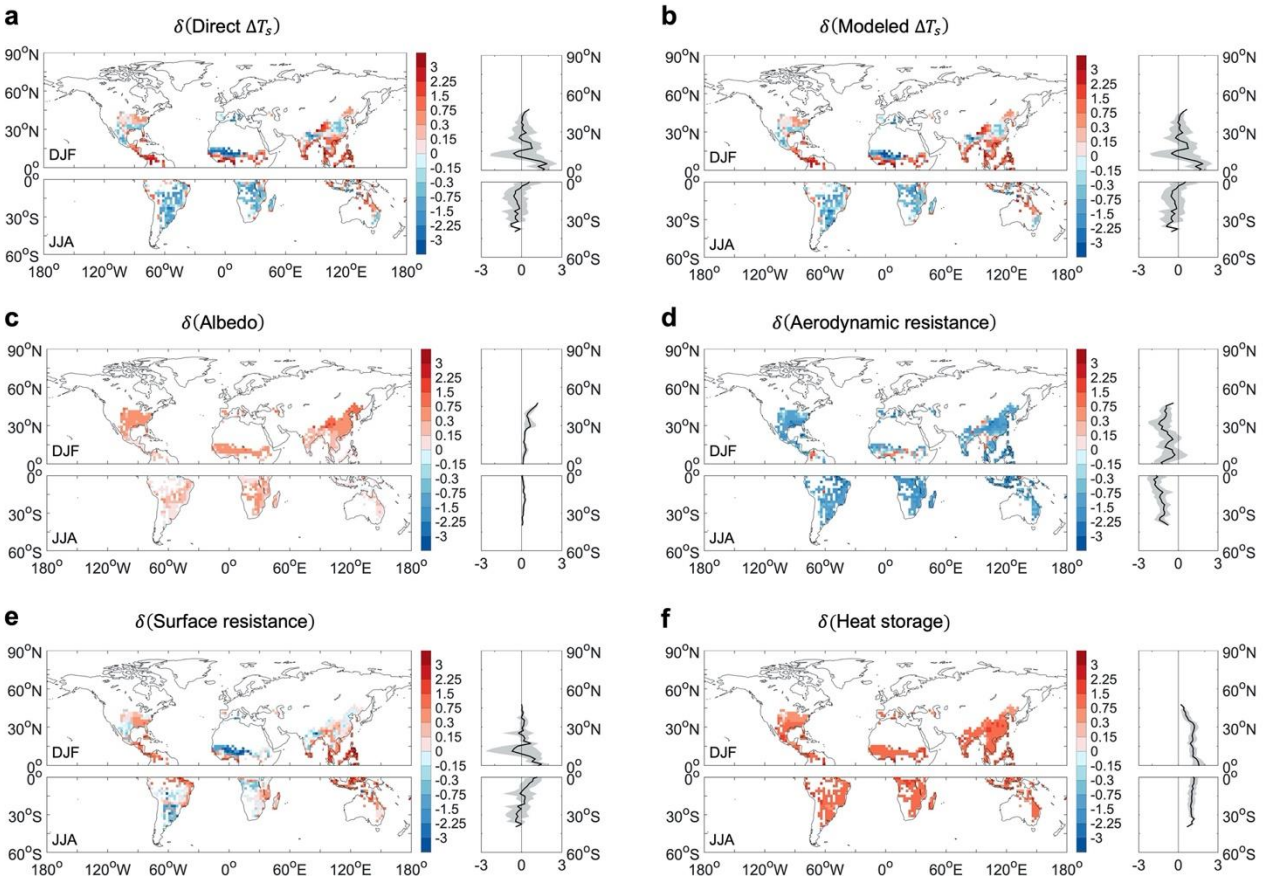

FIG. S7. Differences (δ) in the attribution results between the GFDL ESM2Mb and the CESM models (GFDL minus CESM) during winter. Units are ºC.

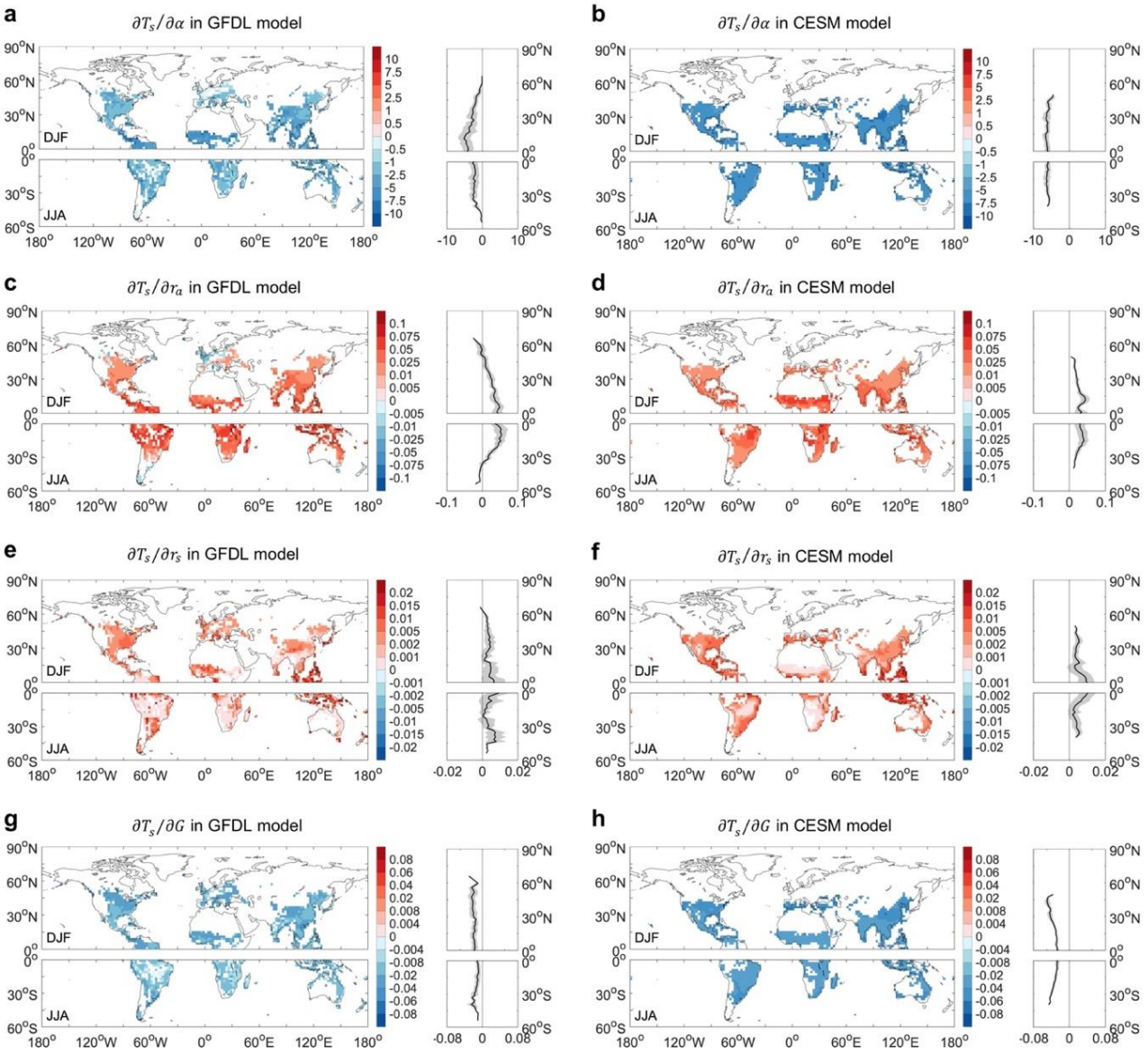

FIG. S8. A comparison of the sensitivities of LST to albedo ($\partial T_s/\partial\alpha$), aerodynamic resistance ($\partial T_s/\partial r_a$), surface resistance ($\partial T_s/\partial r_s$), and heat storage ($\partial T_s/\partial G$) in the GFDL ESM2Mb and the CESM models during winter. Left column corresponds to the results in the GFDL ESM2Mb model, while right column corresponds to the results in the CESM model. Units are ºC for $\partial T_s/\partial\alpha$, ºC m s^{-1} for $\partial T_s/\partial r_a$ and $\partial T_s/\partial r_s$, and ºC m^2 W^{-1} for $\partial T_s/\partial G$.

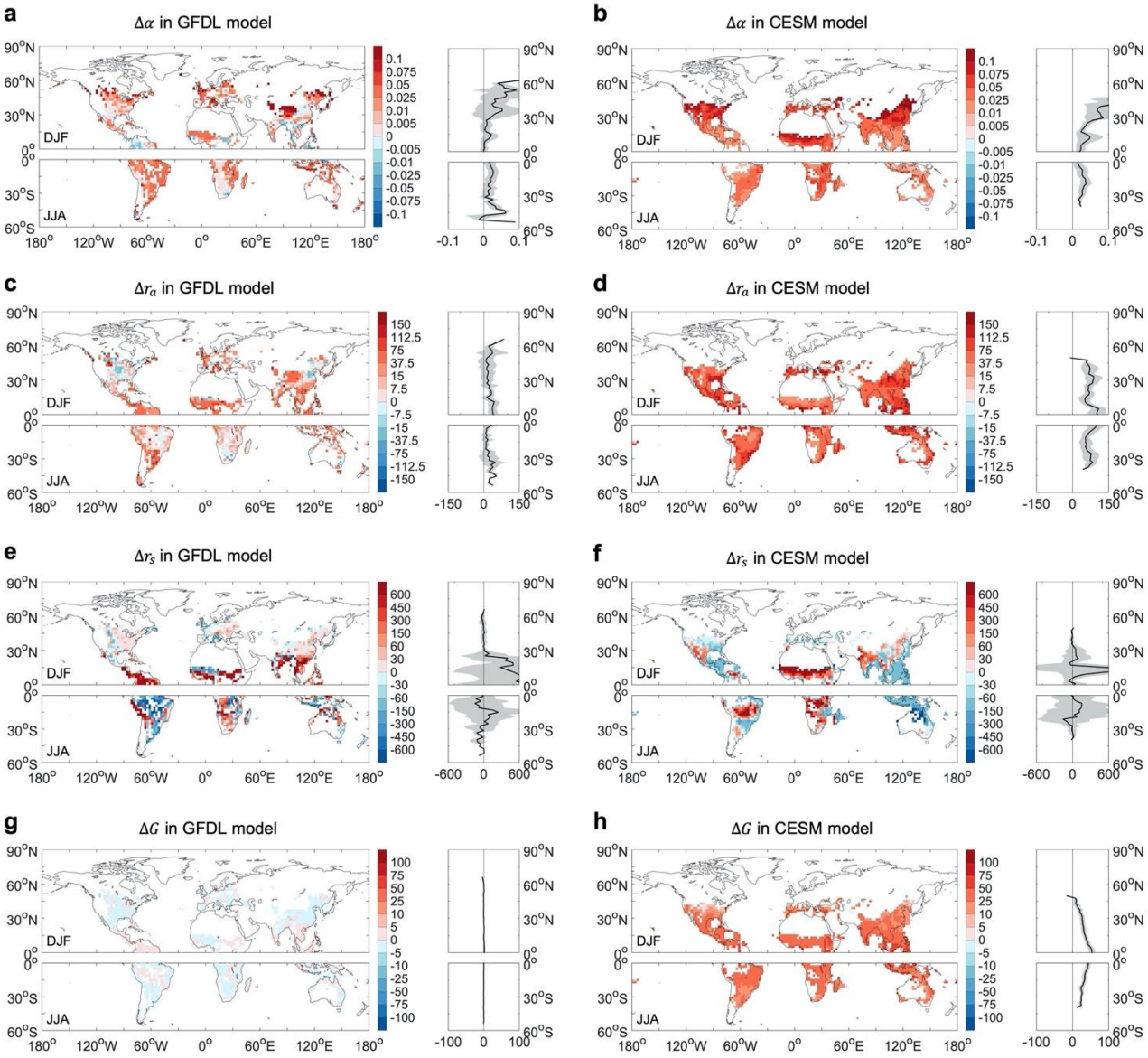

FIG. S9. A comparison of the changes (Δ = cropland – forest) of albedo ($\Delta\alpha$), aerodynamic resistance (Δr_a), surface resistance (Δr_s), and heat storage (ΔG) in the GFDL ESM2Mb and the CESM models during winter. Left column corresponds to the results in the GFDL ESM2Mb model, while right column corresponds to the results in the CESM model. Units are / for $\Delta\alpha$, s m^{-1} for Δr_a and Δr_s, and W m^{-2} for ΔG.

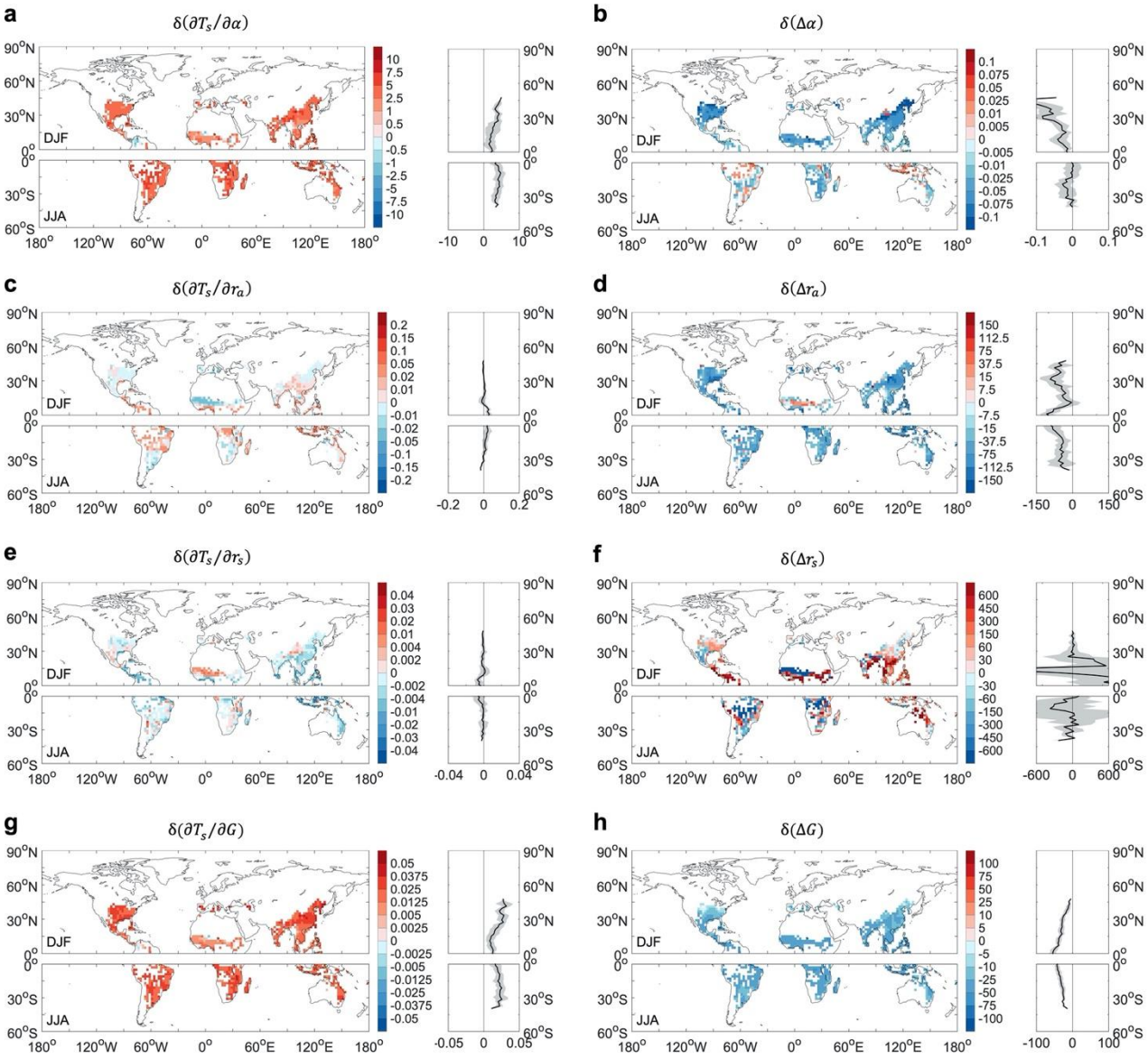

FIG. S10. The differences (δ) in terms of the sensitivities and the biophysical changes between the GFDL ESM2Mb and the CESM models (GFDL minus CESM) during winter.

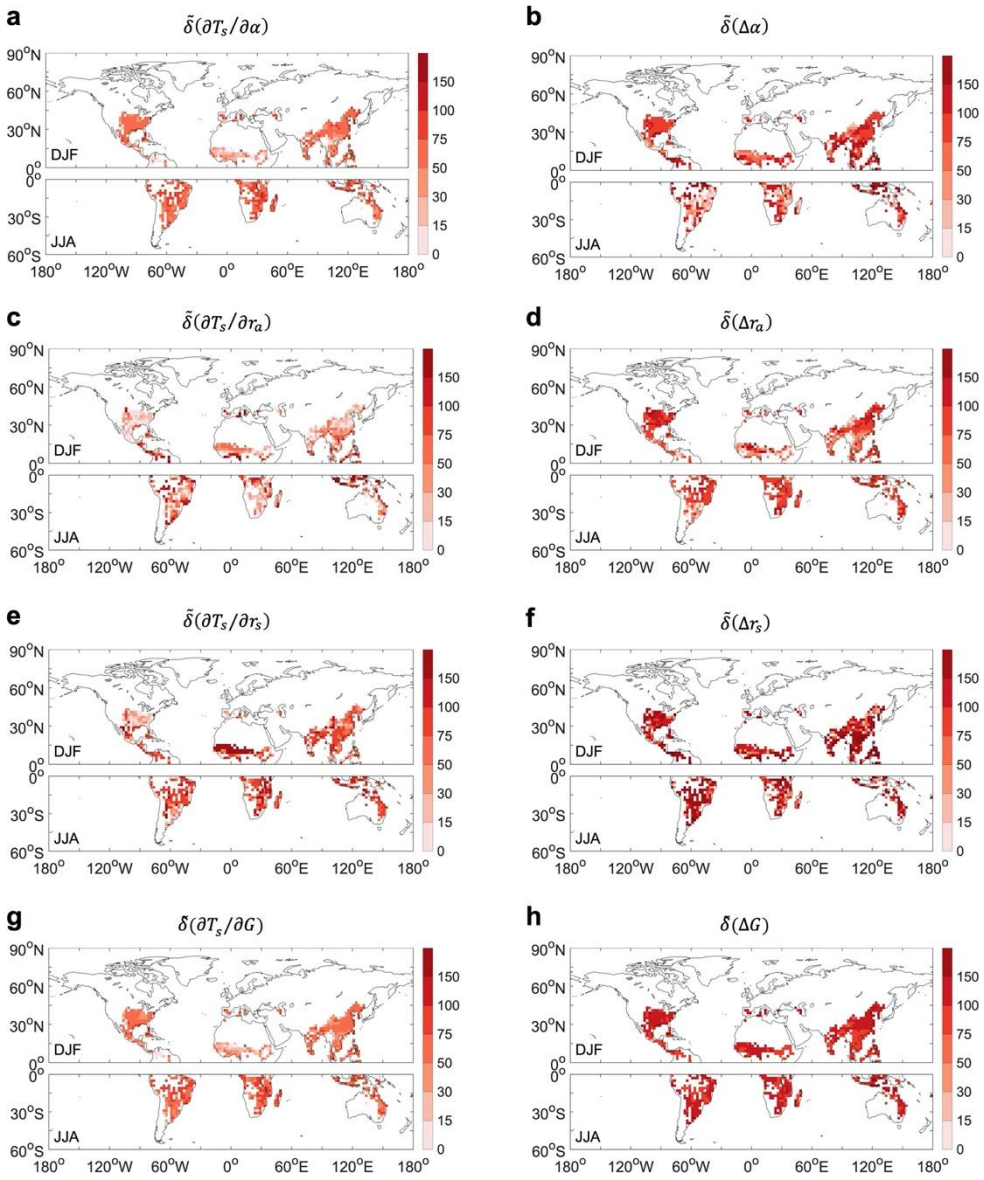

FIG. S11. The fractional differences (δ) in terms of the sensitivities and the biophysical changes between the GFDL ESM2Mb and the CESM models during winter. Units are %.

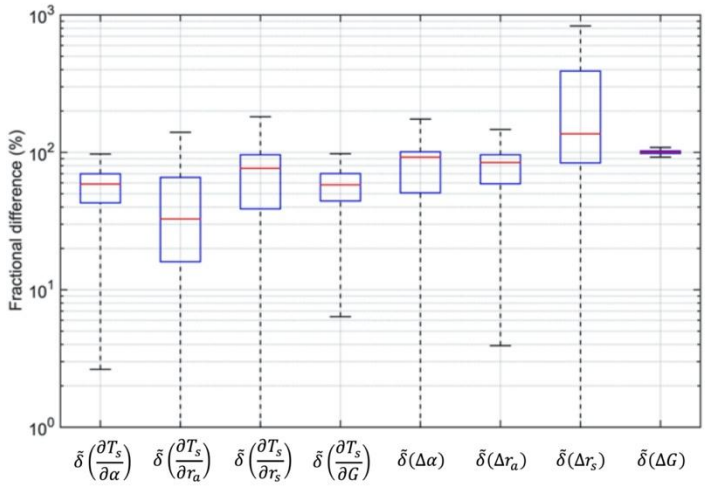

FIG. S12. Boxplots of the fractional differences (δ) in terms of the sensitivities and the biophysical changes during winter.